

Cauê P. Carvalho<sup>\*1</sup>, João P. Pascon<sup>1</sup>, Milton S. F. Lima<sup>2</sup>, Carlos A. R. P. Baptista<sup>1</sup>

<sup>1</sup>Engineering School of Lorena, University of São Paulo (EEL/USP), Lorena/SP, Brazil (\*email: caue.pc@usp.br);

<sup>2</sup>Institute of Advanced Studies, Department of Aerospace Science and Technology (IEAv/DCTA), São José dos Campos/SP, Brazil.

Acknowledgements:



## Abstract

Laser heating treatment (LHT) is a residual-stress-based approach exhibiting successful results in reducing fatigue crack propagation rates in laboratory specimens. Although its effect is usually related to the original residual stress field, it is known that cyclic loading and crack growth can cause relaxation and redistribution of residual stresses. In this work, M(T) specimens made of 2.0 mm thick AA2198-T851 alloy sheets with L-T and T-L crack orientations were treated with a fibre laser (power 200 W, displacement speed 1 mm/s) to produce two heating lines ahead of each crack front on one of each specimens' face. Constant-amplitude loading tests were conducted on treated and untreated specimens at a zero-to-tension condition ( $R = 0$ ). In addition, electrical resistance strain gauges bonded 4 mm away from the notch tip along the crack path were employed to measure the deformation behaviour ahead of the approaching crack tip. A numerical model was developed for the stress-strain state ahead of the crack, including plane stress condition, linear elastic response, the anisotropic Gurson-Tvergaard-Needleman (GTN) yield criterion coupled with damage, associative plastic flow rule and nonlinear isotropic hardening Swift model. The mesh refinement was concentrated around the crack path direction from the notch tip until the specimen's edge. The experimental results showed significant fatigue crack growth (FCG) retardation experienced by the laser-treated specimens; this effect was more pronounced in the L-T orientation. Numerical simulations could depict the stress field distribution in the treated specimen. Numerical simulations of damage increment under monotonic loading were adopted for a preliminary evaluation of the effect of LHT on the strain behaviour of the specimens.

## Introduction

**Laser heating treatment (LHT)** is a residual-stress-based technique consisting of local heating, arising from the interaction between the laser beam and the material in a continuous line, followed by fast cooling. Similar to weld behaviour, the heated area associated with the laser incidence promotes tensile residual stresses. However, in the surrounding area, a compressive residual stress field is formed. The technique had its potential in retarding FCG in aeronautical aluminium alloys emphasized in the past decade [1-3].

Schnubel et al. [1] observed the beneficial effect of LHT on fatigue crack growth (FCG) behaviour of 5 mm thickness C(T)100 specimens out of the AA2198-T8 alloy. Similarly, Growth et al. [2] noticed the technique's benefits on more reliable specimens, the M(T)200, in AA 2024-T3 of 2 mm thickness. **The current work authors** presented the technique's positive effect on AA2198-T851 [3], also evidencing that this effect was more pronounced in lower R-ratio values.

For the matter of numerical analysis, the anisotropic **Gurson-Tvergaard-Needleman (GTN) yield criterion coupled with damage** was originally introduced by Gurson [4] and subsequently improved by Tvergaard [5] and Tvergaard and Needleman [6]. This model is based on a plastification criterion that incorporates the influence of mean stress, as well as ductile damage, measured as the volumetric percentage of discontinuities on the material.

## Experimental Procedure

**Table 1:** Experimental procedure parameters and corresponding equipment detail.

Procedure	Parameters	Equipment detail
Laser heating process	Power: 200 W; scanning speed: 1 mm/s; focal diameter: 2 mm.	IPG Photonics Yb: fibre laser, model YLR-2000, with a maximum power output of 2kW
Fatigue crack growth test	$F_{max} = 6$ kN; $f = 5$ Hz; $R = 0$ ; sinusoidal wave under force control	MTS 810 servo-hydraulic machine; clip gauge MTS mod. 632.03F-21
Strain gauge bonding	Position: 9 mm from specimen centre; Resistance: 120 $\Omega$ ; k-gauge factor: 1.73	Half-bridge HBM LY43-0.6/120 linear strain gauges
Strain gauge data acquisition	Acquisition frequency: 1200 Hz (over 200 points per loading cycle)	QuantumX MX840A universal amplifier, assisted by the catmanEasy software

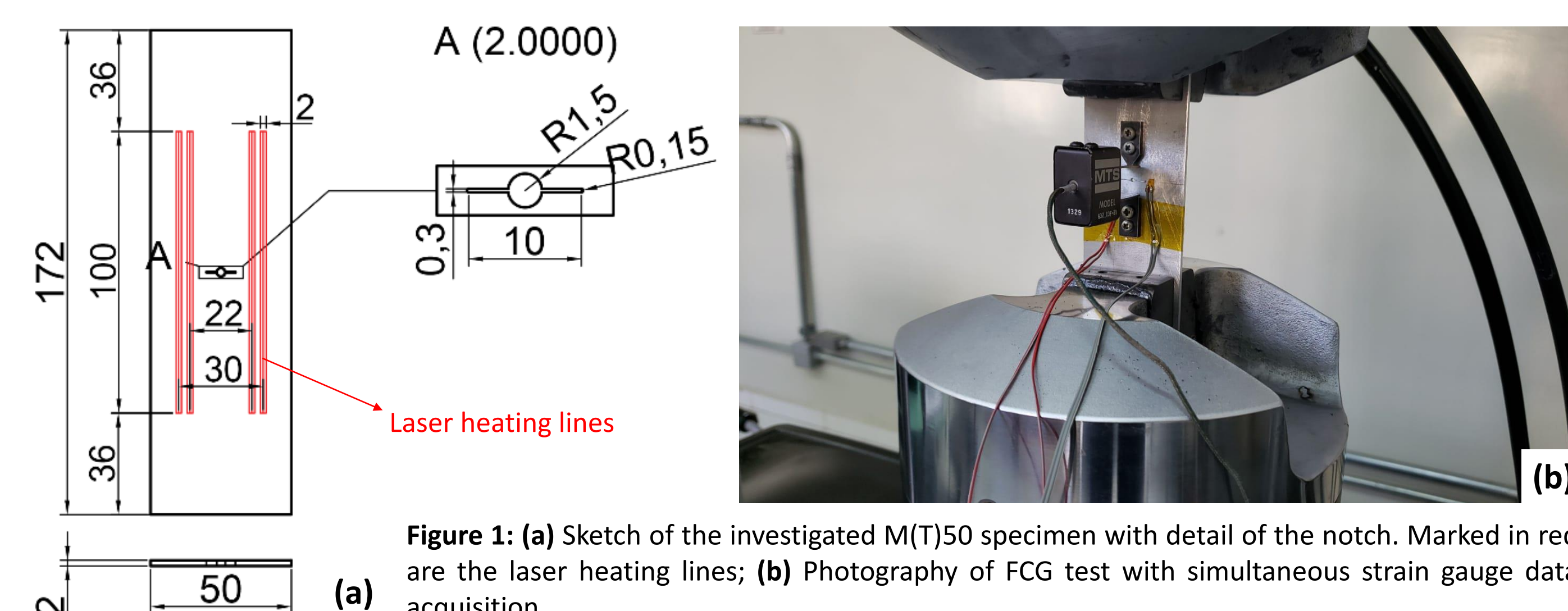


**Figure 1:** (a) Sketch of the investigated M(T)50 specimen with detail of the notch. Marked in red are the laser heating lines; (b) Photograph of FCG test with simultaneous strain gauge data acquisition.

## Numerical Analysis

**Table 2:** Material coefficients employed in the numerical simulations.

Model	Parameters	Unit	Equation
Swift	$K = 423.63$ $\epsilon_0 = 0.00380602$ $n = 0.0549$	MPa - -	$h = K(\epsilon_0 + \kappa)^n$
Yield criterion	$q_1 = 1.5$ $q_2 = 1.0$ $f_0 = 0.01$ $f_c = 0.04$	- - - -	$\sigma_{VM} = \sqrt{1 + (q_1 f)^2 - 2q_1 f \cosh\left(\frac{3q_2 p}{2\sigma_Y}\right)} \sigma_Y \leq 0$
Damage evolution	$f_N = 0.001$ $s_N = 0.3$ $\epsilon_N = 0.1$	- - -	$\dot{f} = \dot{f}_{gr} + \dot{f}_{nuc}$ $\dot{f}_{gr} = (1-f)tr(\dot{\epsilon}_p)$ $\dot{f}_{nuc} = \frac{f_N}{s_N \sqrt{2\pi}} \exp\left[-\frac{1}{2} \left(\frac{\kappa - \epsilon_N}{s_N}\right)^2\right]$
Viscoplasticity	$B_0 = 0.00167$ $m = 14$ $\delta = 0.5$	1/s - -	$\dot{\kappa} = g_0 \left(\frac{\sigma_Y}{h s}\right)^m$
Thermal softening	$T_0 = 295$ $k_T = 1000$	K K	$s = 1 - \delta \left[ \exp\left(\frac{T - T_0}{k_T}\right) - 1 \right]$
Thermal dilatation	$\alpha = 0.000023$	1/K	$\dot{\epsilon}_t = \alpha \Delta T$
Thermal coefficients	$\hat{\epsilon} = 920$ $\chi = 0.9$ $\rho = 2700$ $C_T = 204$	J/kg K - kg/m <sup>3</sup> W/m K	$\rho \hat{c} \dot{T} = \chi W_p - C_T \nabla^2 T$

The thermoviscoplastic GTN ductile damage model has been implemented in a computer code using **2D linear-order triangular finite elements**. Half of the specimen has been discretized, resulting in a mesh with **440 nodes** and **822 finite elements**.

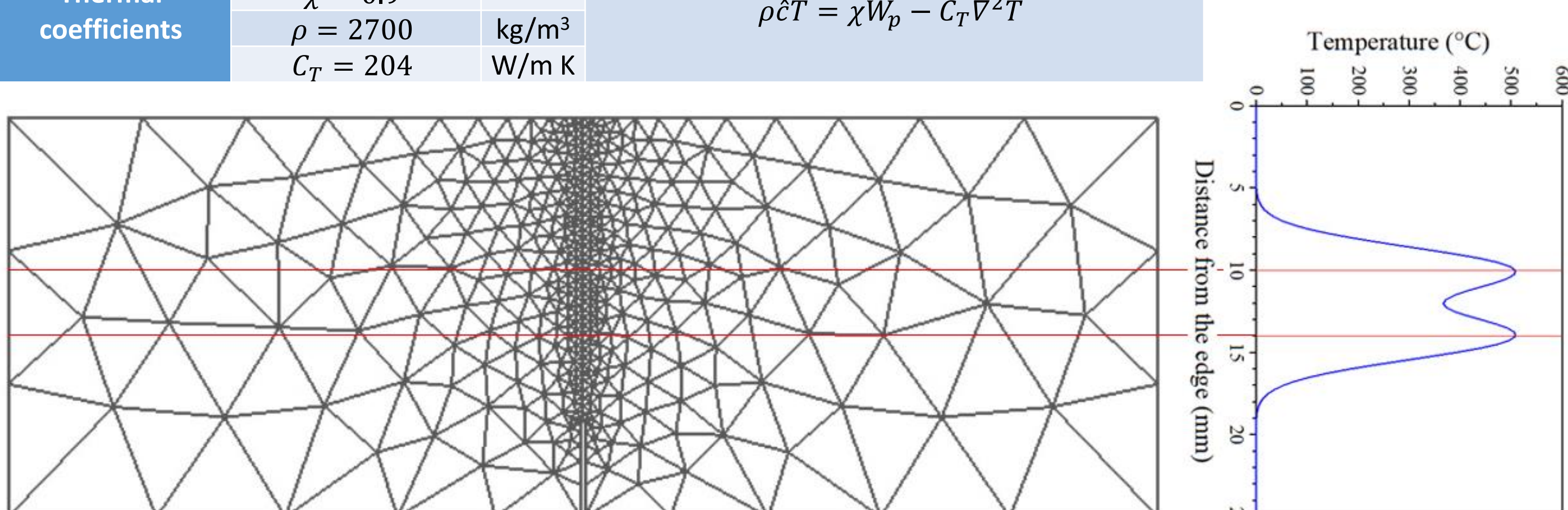


**Figure 2:** Discretization adopted together with the temperature distribution. The peaks at the graph correspond to the position of the laser lines ( $x=10$  mm and  $x=14$  mm).

## Results and Discussion

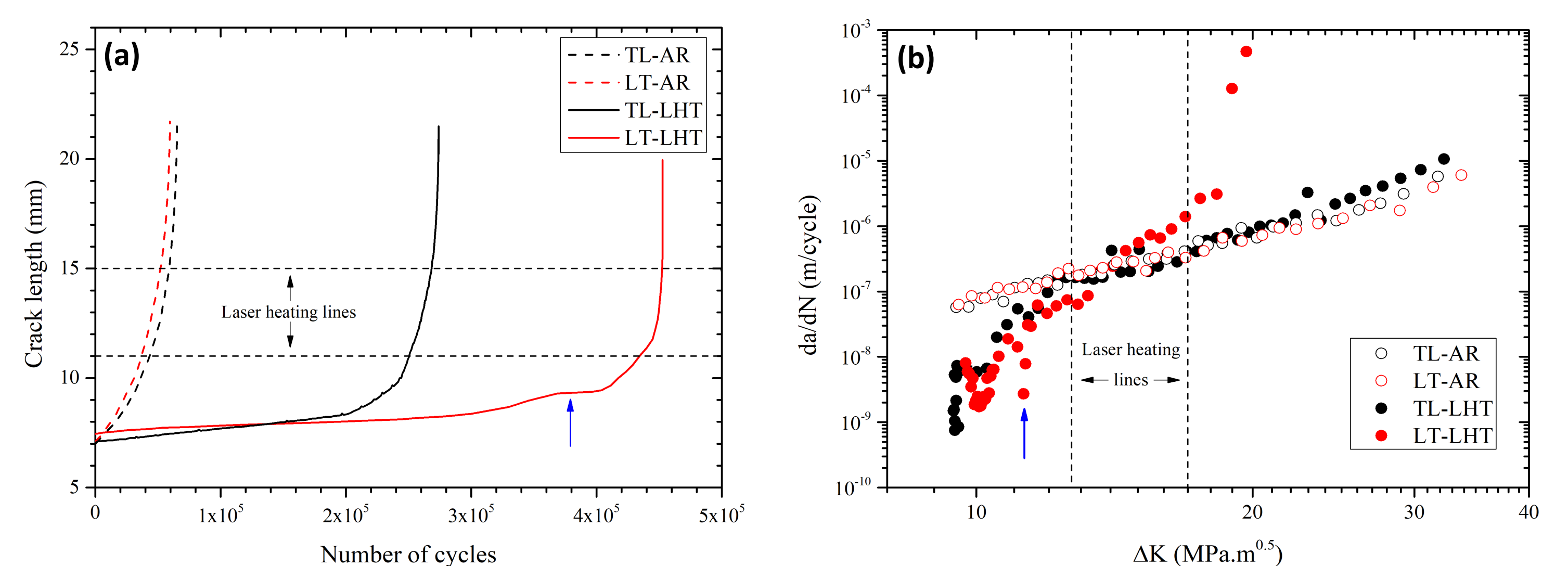


**Figure 3:** (a) Crack length versus the number of cycles' curves; and (b)  $da/dN$  versus  $\Delta K$  of cycles curves of L-T and T-L specimens, for both as-received (AR) and laser heat treated (LHT) conditions.

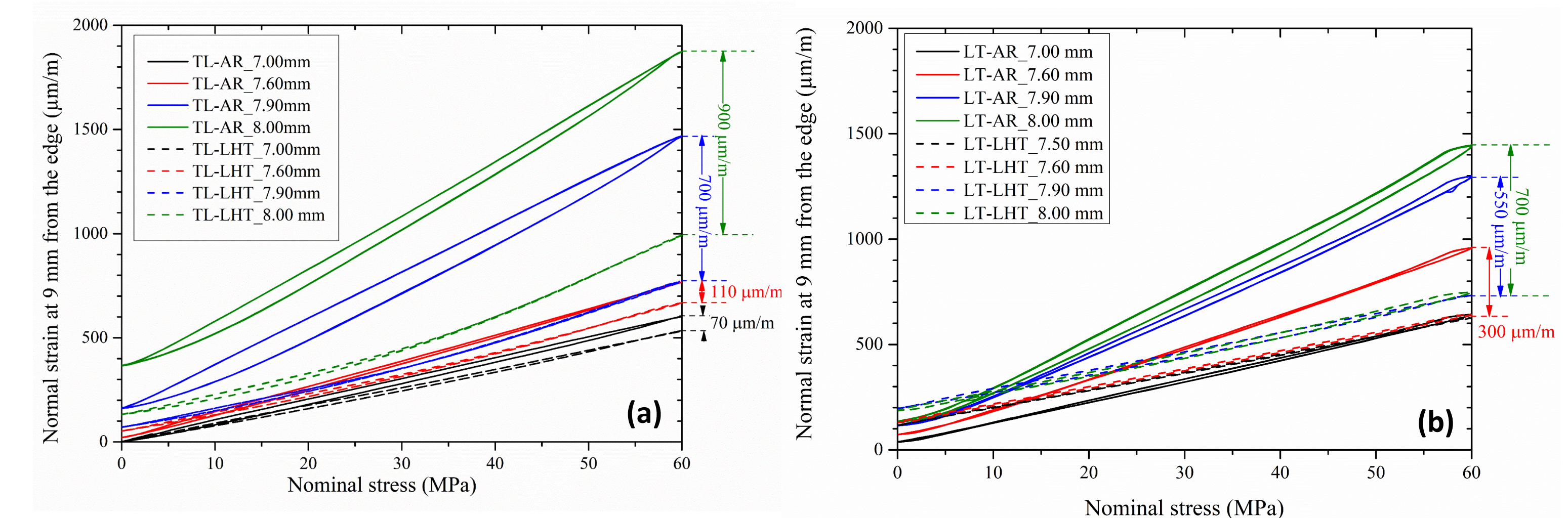


**Figure 4:** Hysteresis loops evaluating AR and THL conditions for different crack sizes. (a) Represents TL specimens; and (b) LT ones.

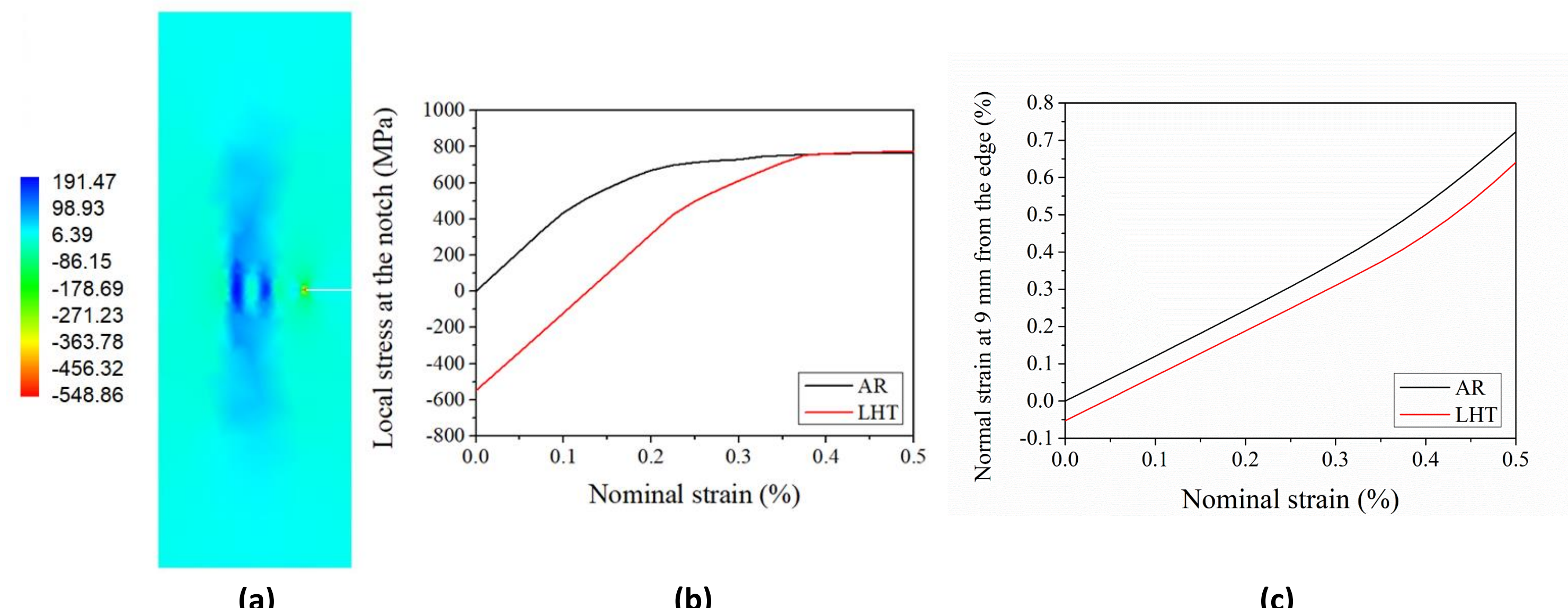


**Figure 5:** Normal stresses (MPa) along the loading direction: (a) distribution of residual stresses at the end of the heating/cooling stage (LHT condition); (b) evolution of stress at the notch tip for both AR and LHT conditions; (c) evolution of the normal strain along the loading direction at the point located 9 mm from the right edge of the specimen.

## Conclusion

- Both AA2198-T851 LT and TL specimens with LHT exhibited an increase in lifespan greater than 300%, with the effect in the former crack orientation being more noticeable;
- $da/dN \times \Delta K$  curves indicate that LHT effect on FCG is more pronounced before the crack front achieves the first heating line, after this point, treated specimens follow the same trend as the AR ones;
- The numerical analysis points out that tensile residual stresses are present in the heating lines, but compressive ones are exhibited in the surroundings, with the latter greater on the notch tip (around 550 MPa);
- The numerical analysis on both the crack tip and 9 mm from the specimen's edge is a first glance at how LHT specimens behave under submitted loading (monotonic loading in this case);
- Strain gauge data provided initial information regarding the redistribution of residual stresses, highlighting how the LHT causes the normal strain values to decrease for the same crack sizes, compared to the AR condition

## References

- [1] Schnubel, D., Horstmann, M., Ventzke V., Riekehr, S., Staron, P., Fischer, T. and Huber, N. (2012), *Materials Science and Engineering A*, vol. 546, p. 8-14.
- [2] Groth A., Horstmann M., Kashaev N. and Huber N. (2015), *Procedia Engineering*, vol. 114, p. 271-276.
- [3] Carvalho, C. P., Lima, M. S. F., Pastoukhov, V. and Baptista, C. A. R. P. (2021), *Metals*, vol. 11, p. 2034.
- [4] Gurson, A. L. (1977), *Journal of Engineering Materials and Technology*, vol. 99, p. 2-15.
- [5] Tvergaard V. (1982), *International Journal of Fracture*, vol. 18, p. 237-252.
- [6] Tvergaard V. and Needleman, A. (1984), *Acta Metallurgica*, vol. 32, p. 237-252.